# Study of the Aluminophosphates $AlPO_4$-21 and $AlPO_4$-25 by $^{27}Al$ Double-Rotation NMR

**R. Jelinek,[‡] B. F. Chmelka,[†,‡] Y. Wu, P. J. Grandinetti,[‡] A. Pines,*[,‡] P. J. Barrie,[§] and J. Klinowski[§]**

*Contribution from the Materials Sciences Division, Lawrence Berkeley Laboratory and Department of Chemistry, University of California, Berkeley, California 94720, and Department of Chemistry, University of Cambridge, Lensfield Road, Cambridge CB2 1EW, U.K.*
*Received October 29, 1990*

**Abstract:** Aluminum-27 double-rotation NMR in a magnetic field of 11.7 T distinguishes the extremely distorted five-coordinated aluminum sites in the molecular sieve precursor $AlPO_4$-21. Upon calcination, $AlPO_4$-21 transforms to $AlPO_4$-25, which has two tetrahedral aluminum sites with similar isotropic chemical shifts that cannot be resolved in an 11.7 T field. The two tetrahedral environments, however, have different quadrupole coupling constants and are distinguished by double rotation at 4.2 T field. The quadrupole coupling constants obtained for these sites indicate that the tetrahedral aluminum environments are less distorted in the hydrated material.

## Introduction

The development of double rotation (DOR) and dynamic angle spinning (DAS) represents a useful advance in the study of quadrupolar nuclei by solid-state NMR.[1-4] These nuclei, with spin $> {}^1/_2$, interact not only with magnetic fields but also with electric field gradients. The combination of these interactions produces higher order, orientation-dependent broadening that cannot be removed by magic angle spinning (MAS) or multiple-pulse sequences alone. DOR or DAS, however, average out both the first- and second-order anisotropic interactions. In the DOR experiment the sample is contained inside a rotor, which is itself mounted inside a larger rotor. The big rotor spins about an axis tilted from the magnetic field direction at the conventional "magic angle", 54.74°, the root of the second-rank Legendre polynomial, $P_2(\cos\theta) = 0$, while the angle between the two rotors is 30.56°, the root of the fourth-rank Legendre polynomial, $P_4(\cos\theta) = 0$. Removal of both the first- and second-order anisotropic broadening in this way permits the environment of quadrupolar sites in solids to be probed by NMR with unprecedented detail.

DOR has recently provided new insights into the structural changes undergone by the porous aluminophosphate VPI-5 during adsorption of water;[5] well-resolved $^{27}Al$ DOR resonances are observed for distinct tetrahedral and octahedral environments. In this paper, we examine the aluminum environments in the aluminophosphate $AlPO_4$-21, which is particularly interesting as it contains five-coordinate aluminum in the framework. We also investigate the aluminum sites in both hydrated and dehydrated $AlPO_4$-25, a related molecular sieve.

$AlPO_4$-21 is one of a range of novel crystalline aluminophosphates first synthesized at Union Carbide Laboratories by hydrothermal treatment of gels containing organic templates.[6] Calcination to remove the organic species can produce molecular sieves of potential industrial importance. In the case of $AlPO_4$-21 there is also a structural transition to $AlPO_4$-25 during the calcination process. The structure of $AlPO_4$-21 has been determined by single-crystal X-ray diffraction and is shown in idealized form in Figure 1.[7,8] There are three distinct crystallographic phosphorus sites, which are all regular $P(OAl)_4$ tetrahedra. There are also three distinct aluminum sites: an $Al(OP)_4$ tetrahedron and two distorted five-coordinate $Al(OP)_4(OH)$ environments. The asymmetric charge distribution at the five-coordinated aluminum sites results in large quadrupolar interactions, which cause severe line broadening, making detection of such species particularly difficult with use of conventional MAS methods. It is interesting to note that $AlPO_4$-21 contains Al-OH-Al groups, which is unusual for zeolitic structures. As a consequence, $AlPO_4$-21 comprises three- and five-membered rings as well as the even-numbered rings usually observed in $AlPO_4$ frameworks. It does not, however, violate the Loewenstein rule[9] which only forbids linkages between tetrahedral aluminum atoms.

## Experimental Section

$AlPO_4$-21 was synthesized, according to the general procedure described by Wilson et al.,[6] from a gel containing pyrrolidine as the organic template. The powder XRD pattern obtained for the material verifies the high crystallinity and purity of the $AlPO_4$-21 product. A portion of the $AlPO_4$-21 sample was subsequently calcined in dry oxygen gas at 873 K for 24 h (2 K/min heating rate) to form the molecular sieve $AlPO_4$-25. For recording spectra of dehydrated $AlPO_4$-25, the sample was heated overnight under vacuum at 623 K and transferred into the rotor in a dry nitrogen atmosphere. Conventional $^{31}P$ and $^{27}Al$ MAS spectra were recorded in 4.2 and 11.7 T magnetic fields, by using spinning speeds of 5.5-6.5 kHz. The $^{31}P$ pulse length was 4-$\mu$s, a 90° pulse, while the $^{27}Al$ data were collected by using 3-$\mu$s pulses [90° pulse in solution was 12 $\mu$s]. The recycle delay was 3 s. DOR spectra, also recorded at 4.2 and 11.7 T, were obtained by using a home-built probe that is described elsewhere.[10] The inner DOR rotor was spun at about 5 kHz, and the outer rotor at 600-800 Hz. In the DOR experiments, 1000-2000 acquisitions were obtained by using a 1-s delay between 3-$\mu$s pulses [solution 90° pulse length was 18 $\mu$s]. All spectra were zero-filled to 4K data points, with 100 Hz Gaussian broadening, and referenced to 85% aqueous $H_3PO_4$ for $^{31}P$ and to an aqueous solution of $Al(NO_3)_3$ for $^{27}Al$.

## Results and Discussion

$^{31}P$ and $^{27}Al$ MAS-NMR spectra of $AlPO_4$-21 are shown in Figure 2. The $^{31}P$ MAS spectrum in Figure 2a shows complete resolution of the three distinct phosphorus sites in a population ratio of approximately 1:1:1. The narrow lines at -13.3, -21.1, and -30.3 ppm confirm the high crystallinity of the sample and cover a range of the frequency regime normally associated with

* To whom correspondence should be addressed.
† Current address: Max-Planck-Institut fur Polymerforschung, Postfach 3148, D-6500 Mainz, Germany.
‡ University of California.
§ University of Cambridge.

(1) Llor, A.; Virlet, J. *Chem. Phys. Lett.* **1988**, *152*, 248.
(2) Samoson, A.; Lippmaa, E.; Pines, A. *Mol. Phys.* **1988**, *65*, 1013.
(3) Chmelka, B. F.; Mueller, K. T.; Pines, A.; Stebbins, J.; Wu, Y.; Zwanziger, J. W. *Nature* **1989**, *339*, 42.
(4) Mueller, K. T.; Sun, B. Q.; Chingas, G. C.; Zwanziger, J. W.; Terao, T.; Pines, A. *J. Magn. Reson.* **1990**, *86*, 470.
(5) Wu, Y.; Chmelka, B. F.; Pines, A.; Davis, M. E.; Grobet, P. J.; Jacobs, P. A. *Nature* **1990**, *346*, 550.
(6) Wilson, S. T.; Lok, B. M.; Flanigen, E. M. U.S. Patent 4,310,440, 1982.
(7) Parise, J. B.; Day, C. S. *Acta Crystallogr.* **1985**, *C41*, 515.
(8) Bennett, J. M.; Cohen, J. M.; Artioli, G.; Pluth, J. J.; Smith, J. V. *Inorg. Chem.* **1985**, *24*, 188.
(9) Loewenstein, W. *Am. Mineral.* **1953**, *39*, 92.
(10) Samoson, A.; Pines, A. *Rev. Sci. Instrum.* **1989**, *60*, 3239.

0002-7863/91/1513-4097$02.50/0 

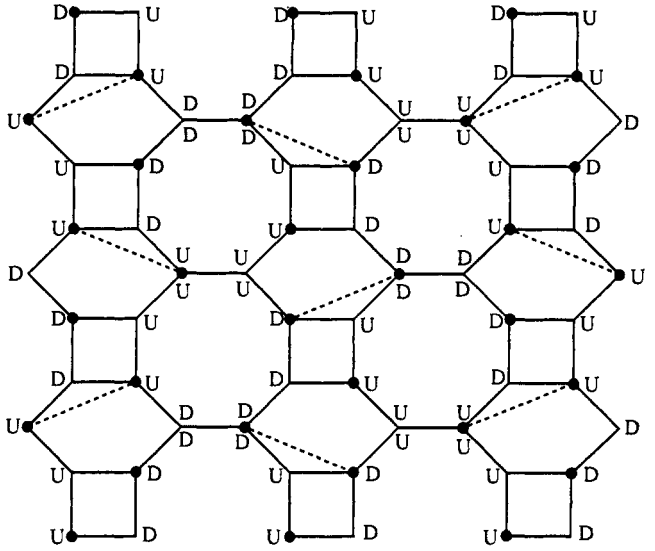

**Figure 1.** Idealized diagram of $AlPO_4$-21 framework. Aluminum atoms are marked by the solid circles, and phosphorus atoms are located at the other vertices. U and D represent upward and downward pointing connections. There is a bridging oxygen in the midpoint of each solid line and a bridging OH group in the middle of the dashed lines which results in two distinct five-coordinate Al sites.

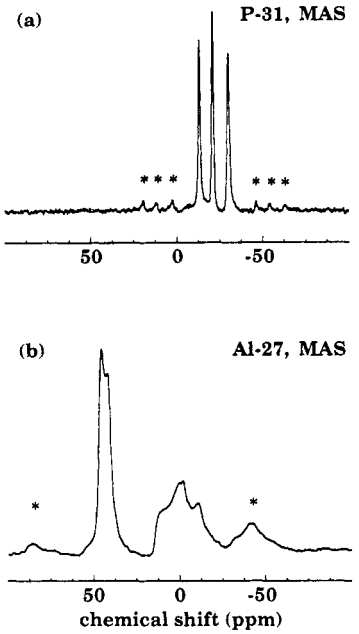


**Figure 2.** MAS-NMR spectra of $AlPO_4$-21 acquired at 11.7 T: (a) $^{31}P$ spectrum, spinning speed 6.5 kHz and (b) $^{27}Al$ spectrum, spinning speed 5.5 kHz.

$P(OAl)_4$ species.[11,12] The correlation suggested by Müller et al.[13] between the $^{31}P$ chemical shift and the mean P–O–Al bond angle in $AlPO_4$ polymorphs enables these peaks to be assigned to specific crystallographic sites. We have calculated the P–O–Al bond angles in pyrrolidine-containing $AlPO_4$-21 from the data in ref 7 and assigned the peaks as follows:

$\delta$ = −13.3 ppm, P3 site $\langle$P3–O–Al$\rangle$ = 137.4°

$\delta$ = −21.1 ppm, P2 site $\langle$P2–O–Al$\rangle$ = 142.0°

$\delta$ = −30.3 ppm, P1 site $\langle$P1–O–Al$\rangle$ = 148.8°

The $^{27}Al$ MAS-NMR spectrum shown in Figure 2b features a prominent peak at 44 ppm with a typical second-order quadrupolar broadened line shape, corresponding to the single tetrahedral aluminum environment, and an additional broad signal at lower frequency associated with the two five-coordinated aluminum sites.[14] These resonance lines are broadened by anisotropic second-order quadrupolar effects which are not removed by MAS even at higher spinning speeds.

Better resolution is obtained in the $^{27}Al$ spectrum of $AlPO_4$-21 by using double rotation NMR. Figure 3 shows the $^{27}Al$ DOR spectrum obtained at 11.7 T. DOR averages the second-order quadrupolar interaction to its isotropic component, thus substantially narrowing the peaks. The spectrum shows a single symmetric peak at 42.2 ppm, while two resonances, at 0.4 and −5.4 ppm, due to the five-coordinate sites can be distinguished from the spinning sidebands by varying the spinning speed of the outer rotor. The sideband manifold remains relatively broad, however, making it difficult to quantify the relative amounts of aluminum in each site. The centerband peaks appear at their respective isotropic shifts, incorporating contributions from both the isotropic chemical shift, $\delta_{cs}$, and the isotropic second-order quadrupolar shift, $\delta_{Q,iso}$, as given by

$$\delta_{iso,obs} = \delta_{cs} + \delta_{Q,iso} \quad (1)$$

The isotropic quadrupolar shift $\delta_{Q,iso}$ is related to the asymmetry parameter $\eta$, and the quadrupolar coupling constant $C_Q \equiv \frac{e^2qQ}{h}$, by the equation

$$\delta_{Q,iso}\ (\text{ppm}) = -\frac{3[I(I+1)-\frac{3}{4}]}{40I^2(2I-1)^2}\left(1+\frac{\eta^2}{3}\right)\frac{C_Q^2}{\nu_0^2} \times 10^6 \quad (2)$$

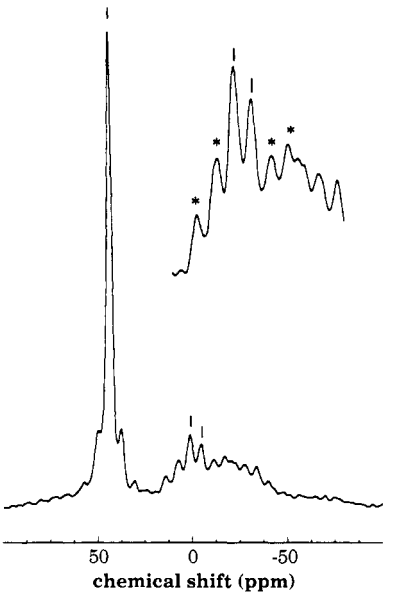


**Figure 3.** $^{27}Al$ DOR spectrum of $AlPO_4$-21 acquired at 11.7 T. The outer rotor was spinning at a speed of 790 Hz.

**Table I.** Parameters Obtained from DOR Results and Simulation of $^{27}Al$ MAS Spectra on $AlPO_4$-21[a]

| site | | $\delta_{iso,obs}$ (ppm) | our MAS simulation $\delta_{cs}$ (ppm) | $\eta$ | $C_Q$ (MHz) | simulation of ref 14 $\delta_{cs}$ (ppm) | $\eta$ | $C_Q$ (MHz) |
|---|---|---|---|---|---|---|---|---|
| Al(1) | $AlO_4$ | 42.2 | 47.3 | 0.15 | 3.7 | 48 | 0.15 | 3.7 |
| Al(2) | $AlO_5$ | 0.4 | 14.6 | 0.68 | 5.9 | 14 | 0.4 | 5.1 |
| Al(3) | $AlO_5$ | −5.4 | 15.7 | 0.52 | 7.4 | 16 | 0.65 | 7.4 |

[a] Isotropic chemical shift, $\delta_{cs}$, asymmetry parameter, $\eta$, and quadrupolar coupling constant, $C_Q \equiv e^2qQ/h$. Our values are compared with those of Alemany et al.[14]

(11) Blackwell, C. S.; Patton, R. L. *J. Phys. Chem.* **1984**, *88*, 6135.
(12) Blackwell, C. S.; Patton, R. L. *J. Phys. Chem.* **1988**, *92*, 3965.
(13) Müller, D.; Jahn, E.; Ladwig, G.; Haubenreisser, U. *Chem. Phys. Lett.* **1984**, *109*, 332.

(14) Alemany, L. B.; Timken, H. K. C.; Johnson, I. D. *J. Magn. Reson.* **1988**, *80*, 427.

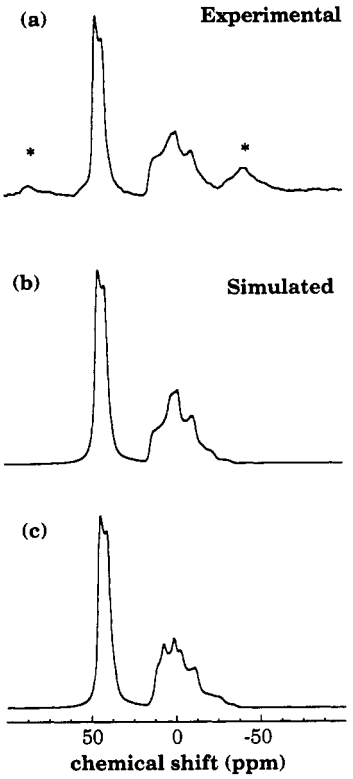


**Figure 4.** $^{27}Al$ MAS spectrum of $AlPO_4$-21 acquired at 11.7 T and MAS computer simulations: (a) experimental, (b) spectral simulation using the parameters given in Table I with site intensity ratio of 1.0:0.3:0.5 [Al(1), Al(2), and Al(3), respectively], and (c) spectral simulation using the parameters given by Alemany et al.[14]

where $I$ is the nuclear spin and $\nu_0$ is the resonance frequency. The DOR results and spectral simulations of the MAS data [Figure 4] yield the quadrupolar parameters for the three sites shown in Table I. It should be pointed out that the parameters obtained by Alemany et al.,[14] upon fast spinning MAS, do not produce a good fit to our experimental data [Figure 4c], although they give a good fit to their experimental spectrum. In particular, our parameters for the five-coordinated site Al(2) are significantly different from those reported previously, though there is good agreement for the other sites. This discrepancy may indicate greater sensitivity of one of the five-coordinate aluminum sites to the method of sample preparation. Our spectral simulation of the centerbands required an intensity ratio of 1:0.3:0.5 for Al(1), Al(2), and Al(3), respectively, which is different from the theoretical 1:1:1 ratio. This difference occurs because of the relatively slow spinning speed—resulting in a significant fraction of the signal from the five-coordinate aluminum to be contained in spinning sidebands. It is possible too that the 3-$\mu$s pulse was not short enough for quantitative analysis of this system, in which the aluminum sites possess substantially different quadrupolar parameters.

The transformation of $AlPO_4$-21 into $AlPO_4$-25 is achieved upon removal of the organic template during calcination. The structure of dehydrated $AlPO_4$-25 above 530 K has been solved recently by Rietveld refinement of neutron time-of-flight data[15] and is shown schematically in Figure 5. This high-temperature form of $AlPO_4$-25 contains the same type of two-dimensional net as depicted in Figure 1 for $AlPO_4$-21 but with an up–down–up–down chain of tetrahedra rather than the up–up–down–down arrangement. This produces two aluminum sites and two phosphorus positions, both of which occur in population ratios of 2:1. At temperatures below 530 K, dehydrated $AlPO_4$-25 appears to adopt a lower symmetry structure.[15] The Rietveld structural refinement showed all aluminum and phosphorus atoms to be tetrahedrally coordinated but was unable to distinguish between them.

(15) Richardson, J. W., Jr.; Smith, J. V.; Pluth, J. J. *J. Phys. Chem.* **1990**, *94*, 3365.

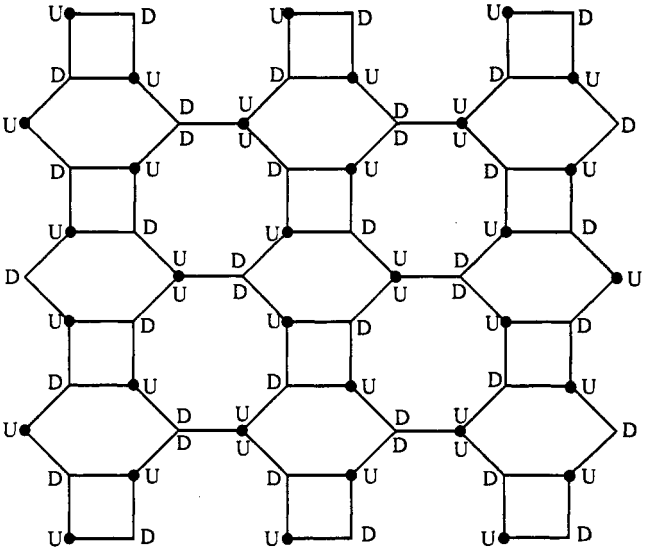

**Figure 5.** Idealized diagram of the $AlPO_4$-25 framework, using the same conventions as in Figure 1.

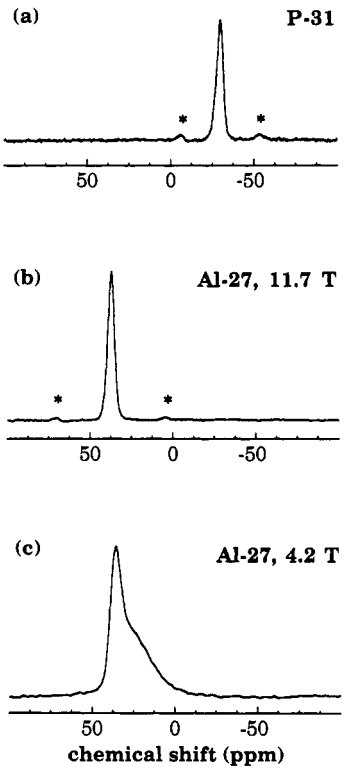


**Figure 6.** MAS–NMR spectra of dehydrated $AlPO_4$-25: (a) $^{31}P$ acquired at 11.7 T, (b) $^{27}Al$ acquired at 11.7 T, and (c) $^{27}Al$ acquired at 4.2 T. The spinning speed for all spectra was 5.5 kHz.

Figure 6 shows the $^{31}P$ and $^{27}Al$ MAS–NMR spectra of dehydrated $AlPO_4$-25. The $^{31}P$ spectrum in Figure 6 acquired at 11.7 T contains a single broad peak at −30.7 ppm, suggesting a range of similar $P(OAl)_4$ environments. The $^{27}Al$ MAS spectra, obtained at 11.7 and 4.2 T [Figure 6 (parts b and c, respectively)], are broadened primarily by second-order quadrupolar effects. The two expected aluminum sites are not resolved in the $^{27}Al$ DOR spectrum of dehydrated $AlPO_4$-25 recorded in an 11.7 T field [Figure 7a]. They are clearly resolved, however, at 21.9 and 33.6 ppm in the DOR spectrum at 4.2 T shown in Figure 7b. The two sites correspond to tetrahedral aluminum and have an intensity ratio of 2:1 as anticipated. The peaks overlap in the higher magnetic field as they have similar isotropic chemical shifts, and their isotropic quadrupolar shifts are comparatively small. Thus, use of lower magnetic fields, for which greater isotropic quad-

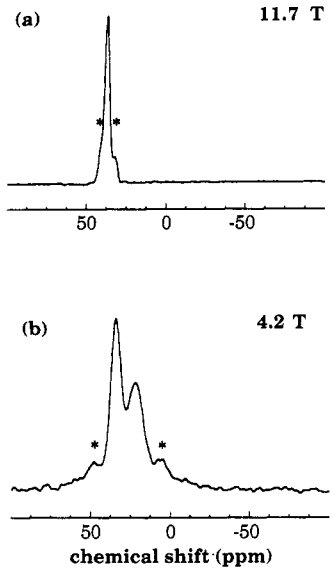


**Figure 7.** $^{27}Al$ DOR spectra of dehydrated $AlPO_4$-25: (a) acquired at 11.7 T and (b) acquired at 4.2 T. Outer rotor spinning speed for both spectra was 750 Hz.

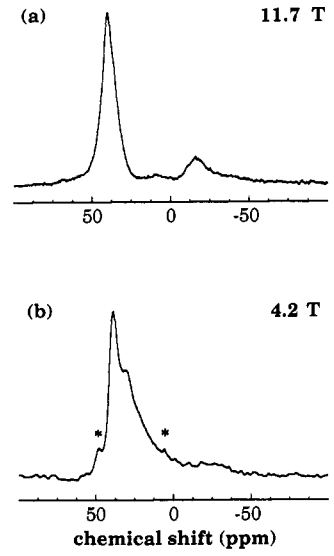


**Figure 8.** $^{27}Al$ DOR spectra of hydrated $AlPO_4$-25: (a) acquired at 11.7 T and (b) acquired at 4.2 T. Outer rotor spinning speed for both spectra was 650 Hz.

rupolar shifts result, may aid the resolution of DOR resonances associated with nuclei in structurally similar sites with small quadrupolar coupling constants. On the other hand, high-field DOR investigations facilitate the interpretation of spectra in cases where quadrupolar nuclei occupy distorted sites of low symmetry for which the quadrupolar coupling constants may be large (>5 MHz).[16] Indeed, the assignment of isotropic peak positions to the five-coordinated aluminum species in $AlPO_4$-21 is possible only at field strengths approaching 11.7 T.

Upon hydration, $AlPO_4$-25 adsorbs approximately 0.145 g of water per 1 g of dehydrated sample. The $^{31}P$ MAS spectrum of hydrated $AlPO_4$-25 was almost identical with the dehydrated material that is shown in Figure 6a. $^{27}Al$ DOR spectra of the hydrated material are shown in Figure 8. At 11.7 T, [Figure 8a], the spectrum contains a main peak at 39.3 ppm, typical of tetrahedral $Al(OP)_4$ species. This tetrahedral peak is broader than the corresponding resonance in dehydrated $AlPO_4$-25 [Figure 7a] due to incomplete overlapping of the two tetrahedral sites as well as embedded spinning sidebands. The broad smaller peak near −16 ppm reflects the existence of octahedrally coordinated framework aluminum bound to adsorbed water. There is a broad resonance at about 10 ppm which indicates the presence of distorted aluminum environments and perhaps extra-framework species. This has also been observed in related aluminophosphates, including VPI-5.[5] Integration of the peak areas indicates that approximately 25% of the framework aluminum sites acquire octahedral coordination upon hydration.

(16) Abragam; A. *Principles of Nuclear Magnetism*; Clarendon Press: Oxford, 1961.

**Table II.** Isotropic Quadrupolar Shifts, $\delta_{Q,iso}$, and Chemical Shifts, $\delta_{cs}$, Calculated for the Two Tetrahedral Aluminum Sites in Dehydrated and Hydrated $AlPO_4$-25[a]

| | dehydrated $AlPO_4$-25 | hydrated $AlPO_4$-25 |
|---|---|---|
| | Site A | |
| | $\delta_{cs}$ = 39.2 ppm | $\delta_{cs}$ = 40.8 ppm |
| 11.7 T | $\delta_{Q,iso}$ = −2.2 ppm | $\delta_{Q,iso}$ = −1.5 ppm |
| 4.2 T | $\delta_{Q,iso}$ = −17.3 ppm | $\delta_{Q,iso}$ = −11.7 ppm |
| | $C_Q$ = 2.3 MHz | $C_Q$ = 1.9 MHz |
| | Site B | |
| | $\delta_{cs}$ = 37.5 ppm | $\delta_{cs}$ = 39.5 ppm |
| 11.7 T | $\delta_{Q,iso}$ = −0.5 ppm | $\delta_{Q,iso}$ = −0.3 ppm |
| 4.2 T | $\delta_{Q,iso}$ = −3.9 ppm | $\delta_{Q,iso}$ = −2.3 ppm |
| | $C_Q$ = 1.1 MHz | $C_Q$ = 0.8 MHz |

[a] The estimates of $C_Q$ take the value of $\eta$ to be 0.67, ensuring an accuracy of ±13%. Measurements were made at two field strengths: 4.2 and 11.7 T.

The $^{27}Al$ DOR spectrum at 4.2 T [Figure 8b] reveals the splitting between the two tetrahedral sites as well as a broad resonance at lower frequency. The positions of the two tetrahedral resonances in the hydrated and dehydrated materials and their isotropic quadrupolar contributions are shown in Table II. We have also estimated the magnitude of the quadrupolar coupling constant by taking the value of $\eta$ to be 0.67, which ensures that $C_Q$ will be correct within 13% [from eq 2]. The quadrupolar shifts are smaller for the hydrated sample than the dehydrated material, showing that hydration confers a more symmetric environment to the tetrahedral sites. This result reflects as well the greater strain in the aluminophosphate framework of the dehydrated form. We also find that different coupling constants exist for the two tetrahedral sites. In Table II, site A corresponds to aluminum at the nodes sharing 6,8- and 8-rings of the framework [see Figure 5]. It is not possible for both the 6- and 8-rings to be regular in the $AlPO_4$-25 structure, and thus the tetrahedron at site A is expected to be quite distorted, accounting for its high quadrupolar coupling constant. Site B corresponds to aluminum sharing 4,6- and 8-rings and will have a more symmetric environment.

The extremely broad resonance between zero and −50 ppm, observed at 4.2 T for the hydrated sample, is assigned primarily to octahedrally coordinated framework aluminum and a range of distorted environments. It is difficult to determine population ratios of the various aluminum sites in hydrated $AlPO_4$-25 owing to the broad line widths. It seems, however, that both tetrahedral aluminum environments in the framework are hydrated to approximately the same extent; the change of the isotropic quadrupolar and chemical shift contributions upon hydration is almost identical for both sites.

## Conclusions

This work demonstrates the use of double rotation in obtaining high-resolution NMR data of quadrupolar nuclei. DOR spectra of $^{27}Al$ species in $AlPO_4$-21 and $AlPO_4$-25 display substantially narrower peaks compared with the second-order quadrupolar broadened line shapes present under MAS conditions. For $AlPO_4$-21, isotropic shifts are obtained for aluminum in one tetrahedral and two five-coordinated environments. The enhanced resolution provided by DOR, combined with MAS spectral simulations, yield quadrupolar parameters for the three sites. During calcination $AlPO_4$-21 is structurally transformed to $AlPO_4$-25, which contains two different tetrahedral aluminum sites that are resolved by DOR at 4.2 T. The tetrahedral aluminum environments conform to higher symmetry upon hydration, relieving the strain present in the framework of the dehydrated material. The water molecules adsorbed produce octahedral aluminum configurations and

probably other distorted environments. In summary, DOR investigations of quadrupolar $^{27}Al$ nuclei, together with $^{31}P$ MAS experiments, yield a wealth of structural information on crystalline aluminophosphates.

**Acknowledgment**. We are grateful to Jay Baltisberger for help with the computer simulation program. This work was supported by the Director, Office of Energy Research, Office of Basic Energy Sciences, Materials and Chemical Sciences Division, U.S. Department of Energy under Contract No. DE-AC03-76SF00098. B.F.C. is a NSF post-doctoral fellow in chemistry. P.J.B. acknowledges financial support from the SERC.

**Registry No.** $AlPO_4$, 7784-30-7.

# Solution Structure and Dynamics of a Mixed Tetramer of Lithium 3,5-Dimethylphenolate and Lithium Perchlorate in Diethyl Ether and Some Related Systems

**L. M. Jackman,* E. F. Rakiewicz, and A. J. Benesi**

*Contribution from the Department of Chemistry, The Pennsylvania State University, University Park, Pennsylvania 16802.* *Received September 28, 1990*

**Abstract:** Lithium 3,5-dimethylphenolate forms a mixed tetramer $Li_4P_3(ClO_4)$ with lithium perchlorate. At temperatures below −20 °C, this tetramer exhibits only one type of phenolate ion in its $^{13}C$ spectrum but two resonances in the ratio of 1:3 in its $^{7}Li$ spectrum. It therefore has cubic tetramer structure **3**. The $^{7}Li$ quadrupole splitting constants for the unique ($Li_U$) and three equivalent nuclei ($Li_E$) are 51 and 133 kHz, respectively, and correspond to a fully solvated tetrameric species. The tendency toward formation of this species depends on the solvent and decreases in the order $Et_2O$ > dioxolane > THF, no mixed tetramer being observed in THF. In dioxolane, some mixed dimer is also formed. Lithium phenolate in dioxolane shows similar behavior. Lithium iodide also forms a mixed tetramer of type **3** in diethyl ether together with a minor amount of a tetramer containing two iodide ions. Contrary to an earlier report, methyllithium forms a mixed tetramer of type **3** with $LiClO_4$ in diethyl ether and this species may be important in reactions with ketones. The first-order rate constants for the intramolecular exchange of $Li_E$ and $Li_U$ and the intermolecular exchange between $Li_E$ and free $LiClO_4$ have been determined. These rate constants are of the order of 1 $s^{-1}$. The rates of exchange between free and bound $ClO_4$ and iodide ions are also of this order.

We have reported[1] that the regiochemistry of the methylation of the tetrameric lithium enolate of isobutyrophenone by methyl *p*-toluenesulfonate (methyl tosylate) in the weakly polar, aprotic solvent dioxolane is profoundly affected by both lithium tosylate, either formed during the reaction or initially added, and added lithium perchlorate. Similarly, we have observed that these salts strongly accelerate the O-methylation of lithium 3,5-dimethylphenolate under the same conditions.[2] Some observations made at the time indicated an interaction between the salts and the tetrameric lithium phenolate and we suggested that the resulting species may be responsible for the change in regiochemistry in the methylation of the enolate ion. The nature of this species was not, however, established but we suspected it might be mixed aggregate, in particular, a mixed tetramer.

Mixed tetramers involving organic lithium compounds have been identified in several systems. Not surprisingly, similarly constituted organolithium compounds, which are themselves prone to form tetramers in weakly polar solvents, form mixed tetramers ($Li_4R_nR'_{4-n}$, **1**) when mixed together. Examples are MeLi/ETLi in diethyl ether,[3] $[LiCH_2Si(CH_3)_3]$/*t*-BuLi in hydrocarbons,[4] and the species **1** (R = BuLi, R′ = PhCCLi, $n$ = 3) in THF.[5] Organolithium compounds also afford mixed aggregates with lithium salts of stronger acids including lithium alkoxides[6,7] and, in particular, with LiBr and LiI. Thus Brown has demonstrated the formation of $Li_4(CH_3)_3I$, $Li_4(CH_3)_3Br$, and $Li_4(CH_3)_2Br_2$ in diethyl ether[8] and has studied the dynamics of interaggregate exchange in the LiBr system.[9] X-ray structures of the mixed aggregates $Li_4R_2Br_2(Et_2O)_4$ (R = cyclopropyl)[10] and $Li_4Ph_3Br(Et_2O)_3$[11] have been reported. We have shown that the lithium enolate of isobutyrophenone forms mixed aggregates of the type $Li_4E_3X$ (X = Cl, Br) in dioxolane, dimethoxyethane, and THF.[12]

There is some evidence, in addition to that cited above, to indicate that the reactivity, regiochemistry, and even stereochemistry of the reaction of mixed tetramers may be significantly different from the parent homoaggregate. McGarrity[13] has convincingly shown that butyllithium/lithium butoxide mixed tetramers are appreciably more reactive than tetrameric butyllithium toward benzaldehyde in THF. Smith has similarly found that lithium ethoxide catalyzes the addition of *sec*-butyllithium to ethyl benzoate in cyclohexane.[14] In contrast, the lithium bromide and iodide mixed aggregates of methyllithium were found to be less reactive than methyllithium to 2,4-dimethyl-4′-(methylthio)benzophenone in diethyl ether.[15] Ashby and Noding[16]

(1) Jackman, L. M.; Dunne, T. S. *J. Am. Chem. Soc.* **1985**, *107*, 2805.
(2) Jackman, L. M.; Petrei, M. M. Unpublished results.
(3) Seitz, L. M.; Brown, T. L. *J. Am. Chem. Soc.* **1966**, *88*, 2174.
(4) Hartwell, G. E.; Brown, T. L. *J. Am. Chem. Soc.* **1966**, *88*, 4625.
(5) Hässig, R.; Seebach, D. *Helv. Chim. Acta* **1983**, *66*, 2269.
(6) McGarrity, J. F.; Ogle, C. A. *J. Am. Chem. Soc.* **1985**, *107*, 1805.
(7) Thomas, R. D.; Clarke, M. T.; Jensen, R. M.; Young, T. C. *Organometallics* **1986**, *108*, 1851.
(8) Novak, D. P.; Brown, T. L. *J. Am. Chem. Soc.* **1972**, *94*, 3793.
(9) Kieft, R. L.; Novak, D. P.; Brown, T. L. *J. Organomet. Chem.* **1974**, *77*, 299.
(10) Schmidbaur, H.; Schier, A.; Schubert, U. *Chem. Ber.* **1983**, *116*, 1938.
(11) Hope, H.; Power, P. P. *J. Am. Chem. Soc.* **1983**, *105*, 5320.
(12) Jackman, L. M.; Szeverenyi, N. M. *J. Am. Chem. Soc.* **1977**, *99*, 4954.
(13) McGarrity, J. F.; Ogle, C. A.; Brich, Z.; Loosli, H.-D. *J. Am. Chem. Soc.* **1985**, *107*, 1810.
(14) Al-Aseer, M. A.; Allison, B. D.; Smith, S. G. *J. Org. Chem.* **1985**, *50*, 2715.
(15) Smith, S. G.; Charbonneau, L. F.; Novak, D. P.; Brown, T. L. *J. Am. Chem. Soc.* **1972**, *94*, 7059.

0002-7863/91/1513-4101$02.50/0 